P13

3D TCAD Simulation of Advanced CMOS Image Sensors

Z. Essa, P. Boulenc, C. Tavernier, F. Hirigoyen, A. Crocherie, J. Michelot, D. Rideau
STMicroelectronics
Crolles, France

Z. Essa
PHELMA Grenoble INP
Grenoble, France

Abstract—**This paper presents a full 3-Dimensionnal TCAD simulation methodology for advanced CMOS image sensors. In order to consider 3D process effects, full 3D TCAD process simulations have been carried out on different advanced pixels. Based upon the obtained 3D doping distributions, 3D opto-electrical device simulation results have been compared to both 2D based approaches and experimental results. Full 3D simulation results show a qualitative agreement with measurements**

Index Terms – Image sensors, 3D simulation, CMOS process, TCAD

I. INTRODUCTION

AS pixel size shrinks in CMOS image sensors market, innovative pixel architectures must be designed in order to follow the fast evolution of the image sensors domain and catch up the needed performances. Some of these new pixels architectures have a fully 3D design. For this reason, TCAD process modelling strategies using 2D simulations [1] or 2.5D simulations [2] (obtained by extending a 2D doping profile simulation into a 3D structure) become inadequate. A new full 3D process and device simulation must be developed to take into account all the 3D effects occurring in the advanced pixels.

In the next section, the different steps that leaded to the new 3D methodology will be exposed. Section III will deal with coupled optical and electrical simulations for various types of advanced pixels.

II. METHODOLOGY

A. Process simulation

Process simulations were performed thanks to Synopsys Sentaurus TCAD dedicated tool (SProcess) [3], which simulates the technological steps of the process including photolithography, etch, deposition, ionic implantation and thermal anneals. Process simulations were made using a continuum approach. The new full 3D methodology for process simulations of semiconductor devices was firstly developed on simple structures such as P/N junctions and MOS transistors.

When comparing 2D and 3D simulated doping distributions, we observed some 3D implantation (shadowing for tilted implants) and diffusion effects close to mask corners on the net doping profile for the simple structures quoted above. During these 3D process simulations we tried to optimize the simulation strategy in SProcess tool, and we had to choose between SDE and MGOALS3D strategies [3]. SDE strategy was preferred for further pixels simulations because it presents the best accuracy-computation time compromise. Meshing engine and parameters were also optimized. Finally, physical models for impurities diffusion, activation and defects clusters were studied in order to choose the most relevant for 3D simulations. Indeed, our CMOS process calibration, based on the default Advanced Calibration of SProcess, gave the best accuracy-computation time compromise.

B. Device simulation

Besides process simulations, device simulations were also optimized for advanced pixels. These simulations used Synopsys Sentaurus TCAD dedicated tool (SDevice) [3] which resolves the Poisson equation and both electrons and holes continuity equations in the structure using a continuum approach. The meshing strategy was chosen material dependant (Silicon, Oxide…) and interfaces dependant (Ex: Silicon/Oxide) to easily manage structures with complex geometry and doping distribution. Meshing strategy accuracy has been compared to a box mesh reference. The comparison was made on several NMOS and PMOS transistors structures used in the 1.4µm pitch pixels studied here and tiny differences were observed.

C. Optical generation

Optical simulations were made using Lumerical Finite Difference Time Domain (FDTD) tool [4] to be coupled to TCAD simulations [2, 5]. The information we want to extract from the optical simulations is the optical generation field defined as the photogeneration rate of electron/hole pairs in silicon (in $m^{-3}.s^{-1}$) and given by:

$$G_{opt} = \frac{-\operatorname{Re}(\vec{\nabla}.\vec{P})}{h\nu} \quad (1)$$

with P the Poynting vector in $W.m^{-2}$, and hν the photon energy. G_{opt} is then injected in the carriers' continuity equations in SDevice [2] as a generation term.

D. TCAD device simulations

Once the optical generation is injected in SDevice tool device simulations can be made on the pixels in order to extract electrical parameters.

The first extracted parameter is the saturation charge Q_{sat} in a given pixel which is defined as the maximum number of charges (electrons or holes) the photodiode can collect. The second extracted parameter is the quantum efficiency versus wavelength QE(λ), defined as the ratio between the number of electrons collected by the photodiode and the number of incident photons for wavelengths between 420nm and 690nm.

III. Coupled Optical/Electrical Simulations Results

A. Front side illuminated pixels

After developing the full 3D methodology, and optimizing process and device simulations, real pixels modelling was carried out. The first simulated pixels are front side illuminated (FSI) and have a 1.4µm pitch with a 3D topography that cannot be approximated by a 2D structure. Fig. 1 presents the pixels 3D simulated structures: left picture presents a Bayer structure [6] and right picture shows an FSI pixel with its doping profile. Note that the colours (red, green and blue) on the top of the pixels are only for the need of visualization.

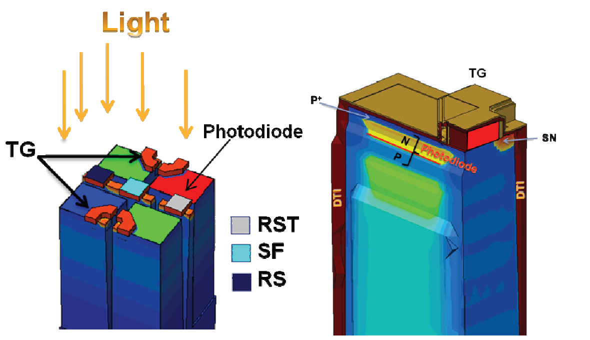

Fig. 1 – Left: 3D simulated Bayer structure of FSI pixels (TG: Transfer Gate, RST: Reset Transistor, SF: Source Follower, RS: Read Select Transistor). Right: 3D simulated doping profile of an FSI pixel (SN: Sense Node, DTI: Deep Trench Isolation)

In front side illumination integration, light crosses the different parts of the sensor back-end (micro-lenses, filters, metal levels) before reaching the active regions in the silicon. On FSI pixels, we simulated the saturation charge Q_{sat} in the Blue pixel by artificially increasing dark current until the photodiode is saturated. Simulated 3D Q_{sat} is 4200 electrons while it is 5800 in both measurements and 2.5D simulations. Such Q_{sat} values were also observed on other kinds of pixels. The mismatch between 2.5D and 3D Q_{sat} simulated result is due to 3D implantation effects. Fig. 2 shows the simulated horizontal photodiode doping distribution for an FSI pixel in 2.5D and 3D. On fig. 2, it can be seen that the 2.5D photodiode is larger than the 3D one which explains the highest Q_{sat} value in 2.5D. As expected, fig. 3 shows that electrons number versus time in the FSI pixel saturates at a higher level in 2.5D than in 3D. To catch the difference between 3D simulated and experimental Q_{sat}, a further calibration should be made on the vertical doping distribution of the pixel in 3D. Indeed, since the 3D photodiode is smaller, one must lower the photodiode vertical pinning to increase the saturation charge.

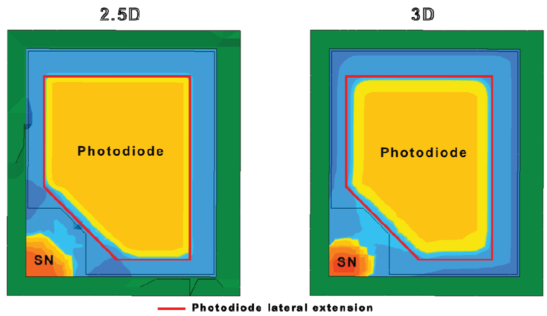

Fig. 2 – FSI pixels photodiode lateral doping distribution: 2.5D (left) and 3D (right) simulated results

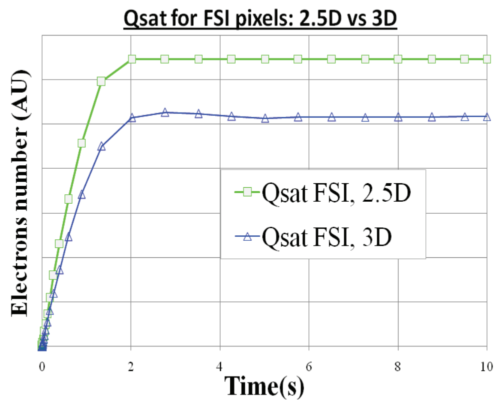

Fig. 3 – Qsat for FSI pixels: 2.5D vs 3D

Fig. 4 shows the quantum efficiency versus wavelength in 2.5D and 3D on a Bayer structure consisting of four FSI pixels with colour filters (R: Red, GR: Green-Red, GB: Green-Blue, B: Blue). QE(λ) results on FSI pixels are quite the same for 2.5D and 3D (Fig. 4) attesting the accuracy of our 3D methodology. However this 3D methodology for process simulations is time-consuming compared to the 2.5D one with a 13/1 time ratio between the 2 methodologies.

Fig. 5 shows measured and 3D simulated QE(λ) curves. Simulated and experimental QE(λ) show the same trend (Fig. 5) with some differences for the maximum for B and R pixels and a small shift for GR and GB pixels. These differences were identified and are due to complex back-end materials characteristics that are not considered in our simulation.

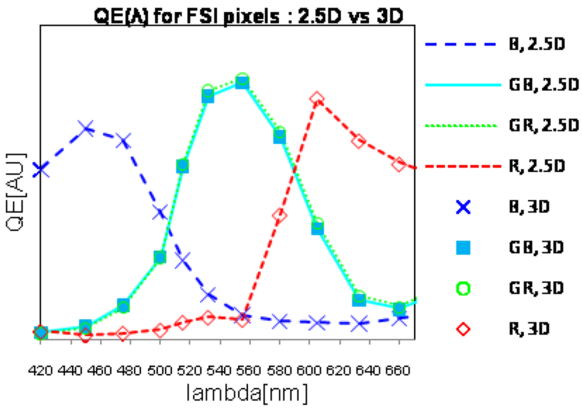

Fig. 4 – FSI pixels QE(λ): 2.5D and 3D simulations results

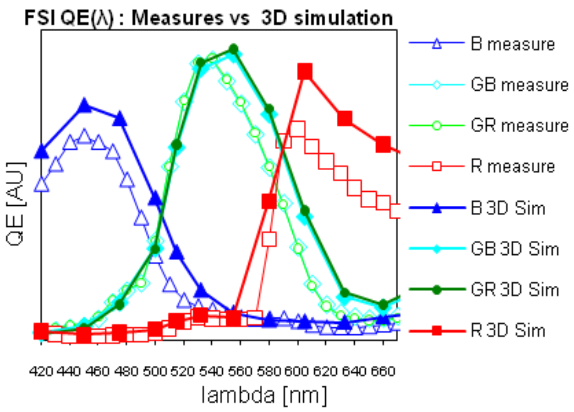

Fig. 5 – FSI pixels QE(λ): measures and 3D simulations results

As we can see, Q_{sat} is more sensitive to 3D effects than QE(λ). While QE(λ) has the same behaviour in 2.5D and 3D (Fig. 4), Q_{sat} is strongly underestimated in 3D (Fig. 3). Actually, Q_{sat} is directly related to the photodiode potential V_{diode} which depends on the lateral and vertical doping distributions in the photodiode. Thus, if the lateral doping distribution is wrongly estimated due to not considered 3D implantation and diffusion effects (Fig. 2 left) as in the case of 2.5D simulations, Q_{sat} value will be strongly affected (Fig. 3). Moreover, if vertical doping distribution is changed, Q_{sat} value will also be affected. Thus, Q_{sat} is a valuable indicator to monitor and calibrate the 3D effects in advanced pixels. On the other side, QE(λ) is much less sensitive to V_{diode} and 3D effects which is confirmed by the entire agreement between 2.5D and 3D simulated results (Fig. 4). This can be explained by the following observations. Firstly, QE(λ) is measured at mid-saturation in the linear regime of the pixel where the photodiode potential well modification is not very strong. Secondly, during QE(λ) measurements, light spot is focalized by a micro-lens on the pixel centre, thus the photodiode lateral extension is less critical.

B. Deep photodiode front side illuminated pixels

Standard pixel architectures have a horizontal planar pinned photodiode which size is related to pixel pitch. Miniaturization of such architectures would lead to smaller photodiodes with lower Q_{sat}. In order to keep Q_{sat} as high as possible, new pixel designs with a vertical pinned deep photodiode have been developed [7]. In such pixels, the photodiode is pinned in all the 3D directions and electrons are stored vertically rather than horizontally. Note that both pixel topography and photodiode extension are fully 3D and their simulation cannot be approximated by any 2D or 2.5D simulation. The deep photodiode front side illuminated pixels (DPFSI) have been simulated with different process conditions. For these different process conditions, the lateral extension of the DPFSI pixel photodiode is reduced/increased which would result in a smaller/higher diode potential. Accordingly, expected Q_{sat} should be reduced (respectively increased) if the photodiode doping lateral extension is reduced (respectively increased) i.e. if lateral pinning is lower (respectively higher). In our simulations, this effect was clearly observed and confirmed lately experimentally.

IV. CONCLUSION

In advanced CMOS image sensors technologies, 3D effects become more and more important because of the 3D topography of small pixels and their 3D doping distribution. Therefore, a full 3D simulation of both pixel process and device is mandatory to catch up such 3D effects. The full 3D methodology presented in this paper was optimized and tested on two different kinds of 1.4µm pitch front side illuminated pixels of advanced image sensors.

The results extracted from electro-optical simulations were similar to those obtained with the previous 2.5D strategy for indicators that are not directly related to the photodiode potential well shape. However, further simulations calibration adjustments are required to match experimental Q_{sat} and QE(λ). Note that this new 3D simulation methodology can be completely extended to back side illuminated pixels where 3D effects are also of main importance. Moreover, this methodology can be adapted to other complex CMOS derivative devices where 3D effects cannot be neglected.

ACKNOWLEDGMENT

The authors would like to thank STMicroelectronics Crolles Optical Simulation team and Imagers Process Integration team for their helpful collaboration during this work.

REFERENCES

[1] C. H. Koo, H. K. Kim, K. H. Paik, D. C. Park, K. H. Lee, Y. K. Park, C. R. Moon, S. H. Lee, S. H. Hwang, D. H. Lee, and J.T. Kong, *"Improvement of Crosstalk on 5M CMOS Image Sensor with 1.7x1.7µm² pixels,"* in Proc. Of SPIE Vol. 6471, 647115, pp. 1-8, 2007.

[2] A. Crocherie, P. Boulenc, J. Vaillant, F. Hirigoyen, D. Hérault and C. Tavernier, *"From photons to electrons: a complete 3D simulation flow for CMOS image sensor,"* in IEEE 2009 Int. Image Sensor Workshop (IISW).

[3] Synopsys TCAD Tools: http://www.synopsys.com/Tools/TCAD.

[4] Lumerical Solutions, Inc. Available: http://www.lumerical.com.

[5] A. Crocherie, *"Modélisation de la diffraction dans les pixels de capteurs d'image CMOS",* thèse CIFRE STMicroelectronics Institut Polytechnique de Grenoble, 2009.

[6] B. E. Bayer, *"Color Imaging Array"*, US Patent n°3971065, Eastman Kodak Company, Rochester, N.Y., July 1976.

[7] J. Michelot, F. Roy, J. Prima, C. Augier, F. Barbier, S. Ricq, P. Boulenc, Z. Essa, L. Pinzelli, H. Leininger, M. Gatefait, J.-E. Broquin, *"Back Illuminated Vertically Pinned Photodiode with in Depth Charge Storage"* in IEEE 2011 Int. Image Sensor Workshop (IISW).